Erosion structures in laminar flumes

Pierre-Yves Lagrée*, Olivier Devauchelle†,**, Khanh-Dang Nguyen Thu-Lam*, Christophe Josserand*, Éric Lajeunesse**, Luce Malverti**, François Métivier ** and Stéphane Zaleski*

*Institut Jean le Rond d'Alembert, CNRS, Université Pierre & Marie Curie, 4 place Jussieu, Paris, France
†Earth, Atmospheric and Planetary Science, MIT, 77 Massachusetts Avenue, Cambridge MA 02139-4307, USA
**Institut de Physique du Globe Paris, Université Pierre & Marie Curie, 4 place Jussieu, Paris, France

Abstract. The present paper is devoted to the formation of sand patterns by laminar flows. It focuses on the rhomboid beach pattern, which may be formed during the backswash. The full incompressible Navier-Stokes equations, with a free surface are coupled with an erodible bed with a bedload transport model, based on a moving-grains balance. A linear stability analysis then shows the simultaneous existence of three types of instabilities, namely ripples, bars and longitudinal striations. The comparison of the bar instability characteristics with laboratory rhomboid patterns indicates that the latter could result from the non-linear evolution of unstable bars.

Keywords: erosion, sedimentation, laminar flow
PACS: 92.40.Gc, 47.20.Ib

INTRODUCTION

On the sea shore (see figure 1) or in sand-bed rivers, one can observe various erosion structures. In many experimental setups (water channels flowing over a bed of small glass beads or sand grains) one can observe the same patterns. For example similar patterns were experimentally obtained by Daerr et al. ([3]), when withdrawing a plate covered with a granular material from a bath of water, at constant angle and velocity.

Shapes are similar even if the flow is laminar instead of turbulent. Some of those structures (see figure 2) are perpendicular to the stream, they are called ripples (and may be considered as two dimensional). Others structures are transverse to the stream (and are then three dimensional), they are diamond-shaped and are called rhomboid erosion patterns. Longitudinal striations may also exist and are parallel to the stream.

The ripple and rhomboid patterns migrate slowly downstream. We claim that most of those structures may be explained by a coupled instability. It means that the fluid flow and the erodible bottom are coupled trough a relation between the shear tress of the fluid (Shields number) and the flux of sediments (this is the erosion law and Exner equation). This erosion flux relation is the least know in the literature, especially over a wavy bed. Depending on the control parameters (Froude Number, slope and aspect ratio of the channel, Shields parameter), and on the chosen erosion law, we show by a linear stability analysis the transition from ripples to various bar instabilities.

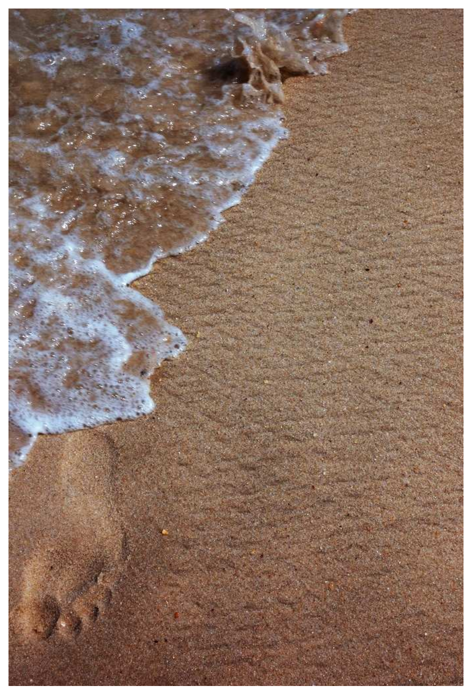

FIGURE 1. Typical see shore diamond-shaped erosion patterns

Finally, we propose experimental evidences of the validity of the theory. The experimental setup consists of a two-meters long inclined channel, which bottom is covered with silica beads. Discrepancies between theory and experiments are discussed. They are mainly due to the lack of any reliable two-dimensions erosion law able to describe the granular flow.

GENERAL MODEL

Fluid flow: full equations

We aim here to study the linear stability of an initially flat sediment layer, as a laminar and steady film of water flows over it. For simplicity, we assume an infinite system both in the direction x of the main slope and in the transverse direction y. The flow in the bulk is given by the stationary and incompressible Navier-Stokes equations in three dimensions,

$$u_k \partial_k u_i = -\frac{1}{\rho}\partial_i p + g_i + \nu \partial_{kk} u_i, \;\; \partial_k u_k = 0, \qquad (1)$$

where u, p and ν are respectively the velocity, pressure and viscosity of water, and g is the acceleration of gravity. The use of stationary flow equations is a common hypothesis in geomorphology, which relies on the idea that the sediment transport time scale is much larger than the flow one. If we neglect both the velocity of the upper layers of grains and the velocity of water through the same layer we may impose the classical no-slip boundary condition at the sediment bed surface in $z = h$ the thickness of the sediment layer. At the free surface, which elevation is denoted by η, both a classical kinematic and a dynamical boundary conditions are imposed.

Sediment transport

We have to write here the conservation law of moving materials due to erosion and sedimentation. This problem has received a large interest recently (Lagrée [6], Valance & Langlois [7]). Basically, one has to write the conservation of mass and momentum for the moving grains, both are reduced in a single conservation equation. As much as possible, we use the notations of Charru [2] in the following. Let us denote by n the density of transported particles per unit surface, then the grains balance in the bedload layer reads :

$$\frac{\partial n}{\partial t} = \dot{n}_e - \dot{n}_d - \frac{\partial q_x}{\partial x} - \frac{\partial q_y}{\partial y}, \qquad (2)$$

where the deposition rate is $\dot{n}_d = c_d U_s n/d_s$ with $c_d = 1/15$ an empirical constant, U_s is the Stokes settling velocity $U_s = (\rho_s - \rho) g d_s^2/(18\rho\nu)$ (ρ_s density and diameter d_s of grains). We then assume that the erosion rate $\dot{n}_e$ is proportional to $(c_g\theta - \theta_t)$ with $c_g = 0.1$. The Shields number is generalized as the ratio $\theta = \frac{||\mathbf{f}^t||}{|f^n|}$ where $\mathbf{f}^t$ is the tangential and f^n the normal component of the force $\mathbf{f}$. This is the total force (viscous force from the flow plus weight) acting on a surface of small area of thickness of the moving grains layer (say $c_g d_s$ which is supposed constant). With these notations, the threshold value remains the one proposed by Charru [2], namely $\theta_t = 0.091$. The choice of the dimensional pre-factors then fixes the empirical constant $c_e = 0.0017$. In the above relation, the slope influence on the tangential shear stress is embedded into the definition of θ. To evaluate the flux, we again follow Charru who observed tha the average particle velocity is proportional to the vertical gradient of the horizontal velocity, times the average flight height. The flux is then obtained by multiplying this average velocity with the suspended particles concentration n:

$$q_x = n c_u d_s \frac{\partial u_x}{\partial z}, \;\; q_y = n c_u d_s \frac{\partial u_y}{\partial z}, \qquad (3)$$

where $c_u = 0.1$ is the third and last empirical parameter of the sediment transport law. We end up with the well-known Exner equation (Exner 1925):

$$C\frac{\partial h}{\partial t} = -\frac{\pi d_s^3}{6}\left(\frac{\partial q_x}{\partial x} + \frac{\partial q_y}{\partial y}\right), \qquad (4)$$

where C is the bed compactness. One should bear in mind that the above equation is a balance for the immobile grains and that it should be used in association with (2).

The above system, from equation (1) to equation (4) could be solved without further assumption. However, to remain consistent with the stationary flow model, we must drop the time derivative in the sediment balance equation (2) but not in (4) as this equation controls the slow topography evolution.

The following section is devoted to the stability analysis of a flat bed within this framework.

Stability

The simplest base state for our system consists in a flat (but tilted) sediment bed, over which flows a uniform layer of water. For low enough values of the Reynolds number (laminar régime), and if we assume that the water velocity vanishes at the granular bed surface, this equilibrium profile driven by the small slope tilt angle S is a parabola:

$$u = U\frac{3}{2}\frac{z-h}{D}\left(2 - \frac{z-h}{D}\right), \qquad (5)$$

where u, z, h and d are the water velocity, the bed elevation and the flow depth and $U = gSD^2/(3\nu)$. This configuration is known as the Nußelt film. The Shields

parameter of this basic flow is denoted Θ.
To describe the flow, the classical non dimensional parameters are introduced: Froude, *Fr*, Bond *Bo*, Reynolds *Re*, they are based on the preceding values.
A normal mode decomposition is done, whe seek for solutions of the form $\bar{f}(\bar{z})e^{i(\bar{k}cos(\phi)\bar{x}+\bar{k}sin(\phi)\bar{y}-\bar{\omega}\bar{t})}$ where $\bar{k}$, ϕ and $\bar{\omega}$ are respectively the wave-vector norm, its angle with respect to the x axis, and the pulsation of the perturbation. The non-dimensional wave vector is nor- malized by D. In the same fashion, the time-scale T for the pulsation is given by the Exner equation:

$$T = \frac{6CD^2}{\pi \ell_d c_d U_s d_s^2 N},\ N = \frac{18 c_e}{c_d d_s^2}(c_g\Theta - \theta_t),\ \ell_d = \frac{3 c_u U d_s}{c_d U_s D},$$

where ℓ_d and N are respectively the deposition length (defined by Charru [2]), and the suspended concentration of the base flow. The deposition length, which corresponds to the order of magnitude of the average flight length of a particle, introduces a space gap between the sediment flux and the shear stress that generates it. This delay stabilizes the perturbations at short wavelengths (see Andreotti et al. [1]; Lagrée [6]).

RESULTS AND DISCUSSION

The sediment transport law employed here is a generalization in three dimensions of the model proposed by Charru [2]. The parameters of the erosion law are provided by this article. We used the flow parameters measured during the experiments for the stability analysis. No additional free parameter was required for our analysis. Solving the dispersion relation gives predictions (pattern angle and wavelength) that are easily measured experimentally. On figure 3 left we plot a typical example of growth rate issued from the numerics. The existence of three distinct maxima is the most striking feature of this dispersion relation. This is not always the case. For other values of the parameters, any association of these three types of maxima is possible, which can makes the distinction uneasy. From these maxima, we will recognize the following patterns:
- Longitudinal striations correspond to maximum nearest to $\phi = \pi/2$ (the mode (a) on figure 3 left). These structures are aligned with the flow, we did observe those structures (though they are not visible on figure 2);
- Ripples correspond to a growth rate maximum lying on the k axis, that is, for $\phi = 0$ (the mode (c) on figure 3 left). These structures are perpendicular to the flow (see figure 2 bottom);
- Bars correspond to any other maximum (the mode (b) on figure 3 left). These structures are inclined with respect to the flow direction, they evolve in diamond patterns.

The value of the angle ϕ usually allows to discriminate between bars and longitudinal striations, the latter being always unstable (in a reasonable range of parameter values).

On figure 3 right we plot an example of comparison with the experimental results of Devauchelle et al. [5]. The comparison concerns the opening angle $\alpha = \pi/2 - \phi$ (in degrees) of the rhomboid pattern. The solid line corresponds to the one-to-one relationship.

This global 3D approach allows to understand how simplified theories may model the flow. For example, on the one hand, there is a large literature on the shallow-water approximation. These equations, named after Adhémar-Jean-Claude Barré de Saint-Venant, are very often implemented in fluvial geomorphology. In fact, these equations do not allow to obtain ripple instabilities but they allow to obtain bar instabilities [4]. A numerical simulation of a reduced linear Saint Venant model for the flow with a non-linear erosion law can be performed. And we can show that this model reproduces the alternate bar instability and leads to the rhombus-shaped pattern. On the other hand, there exists as well a large literature on the stability of erodible beds in a shear flow. In this case, one obtains only transverse ripples ([6],[7]). This present theoretical study provides the bridge between those two simplified approaches.

REFERENCES

1. Andreotti, B., Claudin, P. & Douady, S., Selection of dune shapes and velocities Part 2: A two-dimensional modelling. *The European Physical Journal B-Condensed Matter* **28** (3), 341-352 (2002).
2. F. Charru, Selection of the ripple length on a granular bed sheared by a liquid flow. *Physics of Fluids* **18**, 121508 (2006).
3. A. Daerr, P. Lee, J. Lanuza & É Clément, Erosion patterns in a sediment layer. *Phys. Rev. E* **67**: 065201. (2003).
4. Devauchelle, O. and Josserand, C. and Lagrée, P.Y. and Zaleski, S., Morphodynamic modeling of erodible laminar channels, *Physical Review E*, **76** 5, 56318 (2007)
5. Devauchelle, O., Malverti, L., Lajeunesse, E., Josserand, C., Lagrée, P. -Y. & Métivier, F. Rhomboid beach pattern: a benchmark for shallow water geomorphology. *J. of Geophysical Research* Submitted (2008).
6. Lagrée, P.-Y. A triple deck model of ripple formation and evolution. *Physics of Fluids* **15**, 2355. (2003)
7. Langlois, V. & Valance, A. Formation of Two-Dimensional Sand Ripples under Laminar Shear Flow. *Physical Review Letters* **94** (24), 248001 (2005).
8. Malverti, L., É. Lajeunesse, and F. Métivier, Small is beautiful: upscaling from microscale laminar to natural turbulent rivers, *Journal of Geophysical Research*, in press. (2008),

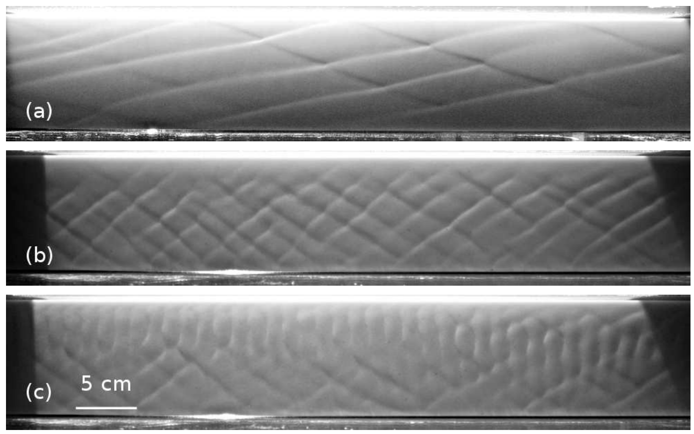

FIGURE 2. Various bedform observed in our experiment. The width of the flume is 10 cm. (a) Large rhom- boid pattern (*Fr* = 1.76, *S* = 0.03, *Bo* = 1.31 and Θ= 0.616). (b) Small rhomboid pattern (*Fr* = 0.95, *S* = 0.015, *Bo* = 3.25 and Θ= 0.485). (c) Rhomboid pattern mixed with ripples (*Fr* = 1.01, *S* = 0.015, *Bo* = 3.50 and Θ= 0.504.

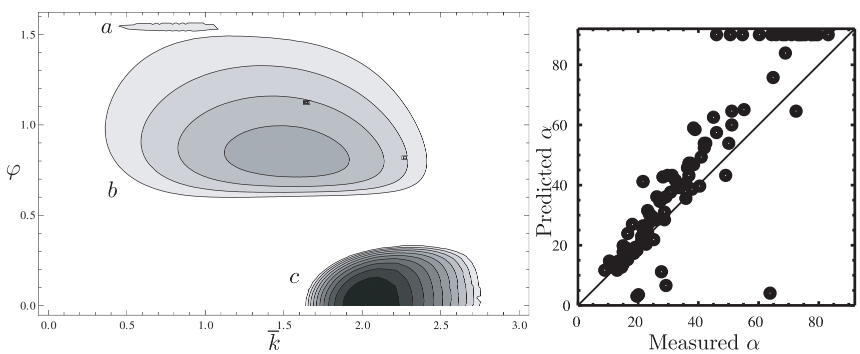

FIGURE 3. Left: Growth rate $Im(\bar{\omega})$ of the tree-dimensional instabilities of a granular bed submitted to erosion by a laminar flow, as a function of the wave-vector norm $\bar{k}$, and angle ϕ with respect to the x direction. The blank domain corresponds to negative values of the growth rate, that is, stable modes. In this typical example, three types of instabilities of different geometrical characteristics can develop: (a) longitudinal striation, which maximum growth rate lies at angle close to $\pi/2$; (b) bar instability, which can occur at any value of the angle ϕ; (c) ripple instability, which crests are perpendicular to the main flow direction, that is, $\phi = 0$. The bar instability is probably responsible for the initiation of rhomboid patterns. In this example, the parameters have values Fr = 0.90, S = 0.015, Bo = 2.77 and Θ = 0.448. **Right:** Comparison between the three-dimensional model of the present paper, and the experimental results of Devauchelle et al. [5]. The comparison concerns the geometrical characteristics of the rhomboid pattern: opening angle $\alpha = \pi/2 - \phi$ (in degrees).